Memory Cell for High-Density Arrays Based on a Multiterminal Superconducting-Ferromagnetic Device

I. P. Nevirkovets* and O. A. Mukhanov
Hypres Inc., Elmsford, New York 10523, USA

(Received 14 November 2017; revised manuscript received 19 June 2018; published 7 September 2018)

We report the fabrication and testing, at 4.2 K, of four-terminal $SIS'F_1IF_2S$ devices, where $S(S')$ denotes a superconductor (Nb), $F_{1,2}$ denotes a ferromagnetic material (Ni and permalloy (Py), respectively), and I denotes an insulator (AlO_x). The F_1IF_2 junction plays the role of a pseudo-spin valve, in which the magnetization vector of the Py layer can be reversed either by an externally applied magnetic field, or, potentially, by the electric current properly supplied to the device. The total magnetic moment of the F_1IF_2 junction, determined by two different magnetization orientations in the F_1 and F_2 layers, can be sensed by an adjacent SIS' junction, resulting in two distinct maximum Josephson critical current values. Such controlled manipulation of the Josephson critical current offers the possibility of building a cryogenic memory cell based on the four-terminal hybrid S/F device. One of the advantages of this memory device is its compatibility with single-flux quantum circuit elements.

DOI: 10.1103/PhysRevApplied.10.034013

I. INTRODUCTION

Over the last several decades, significant research effort has been dedicated to the development of memory for energy-efficient cryogenic computers [1–3]. In particular, various combinations of ferromagnetics and superconductors have been attempted in order to create a cryogenic memory element [4–20]. Some earlier proposals exploited the influence of a stray magnetic field from a magnetic part of the device either on a superconducting stripe [5,6] or a Josephson junction (JJ) [4,7] (we are not aware of any experimental realization of the device [4] by its author). The devices proposed by Clinton and Johnson [5,6] exploit suppression of superconductivity by a fringe magnetic field induced by either one [5] or two [6] ferromagnetic layers; device operation requires driving the superconducting stripe into the normal state.

Oh *et al*. were probably the first to propose a memory concept exploiting a peculiar proximity effect between a superconductor and a ferromagnet [7]. At first sight, their design is similar to that described in Ref. [6]; however, there is an important conceptual difference: the superconducting sensing element changes its state (superconductive or resistive) mainly due to the change of the strength of the proximity effect rather than the net strength of the magnetic field. The strength of the proximity effect depends on the alignment [parallel (P) or antiparallel (AP)] of the magnetic moments of the two magnetic layers, which affects the superconducting transition temperature, T_c, of the superconducting layer. Experimental realizations of this idea have been reported [8,9]. In [9], a full spin switch effect for the superconducting current was achieved for the $CoO_x/Fe_1/Cu/Fe_2/In$ multilayer.

The proposals exploiting the transition of a superconducting layer into a normal state are not well suited for integration with the single-flux quantum (SFQ) logic and for the energy-efficient memory. For easy integration with the SFQ logic that currently dominates superconducting electronics, it is desirable to develop a memory element based on a Josephson junction whose critical current can be reproducibly switched between the two distinct states and maintained as long as necessary in either state. Therefore, these states can serve as logic "0" and "1" states.

Held *et al*. [10] have proposed a memory concept that combines rectangular ferromagnetic dots for the storage of the data and JJs for their readout. Here, the critical current of a JJ is affected by a stray magnetic field induced from a ferromagnetic dot. Since the device comprises a single magnetic element and has lateral geometry, it does not allow for efficient control of the Josephson current and is not well suited for miniaturization.

Samokhvalov *et al*. [11] reported a device in which a Co/Si/Co bilayer magnetic particle was formed on the insulated upper electrode of an *SNS* Josephson junction (where S and N denote a superconductor and a normal metal, respectively). The magnetic state of the particle was set using an externally applied magnetic field above the superconducting critical temperature of the S electrodes, T_c. After cooling the device below T_c, the authors observed the Josephson critical current, I_c, vs externally

*nip13pin@gmail.com

applied parallel magnetic field, H, dependence with a deep minimum near $H = 0$; the dependence was attributed to formation of an Abrikosov vortex-antivortex (V-AV) pair in the top Nb layer of the *SNS* junction as a result of penetration of the fringe magnetic field induced by the magnetic particle. Although this work has demonstrated that a magnetic junction can produce a very strong effect on an adjacent Josephson junction, the device has two drawbacks as a candidate for a cryogenic memory element: first, the magnetic state of the Co/Si/Co junction can only be controlled by an externally applied magnetic field; second, after the V-AV pair is created, it cannot be removed by the application of a weak magnetic field such as the one that reversed the magnetization direction of one of the Co layers, so the I_c magnitude of the Josephson junction cannot be controlled as desired for a memory element.

Larkin *et al*. reported observation of two distinct levels of I_c in $SIS'FS$ magnetic Josephson junctions (MJJs; I denotes an insulator and F a ferromagnetic material) for two magnetization orientations of the F layer where superconductivity was induced by the neighbor S' and S layers [12]. This MJJ geometry was studied in a number of works by the same group (see Ref. [13] and references therein). However, asymmetry in the $SIS'FS$ junctions observed by the authors [12] is due to the self-field effect that will diminish upon reduction of the junction size. In the case of a single F layer, ideally, reversing its magnetization direction will result in a symmetric shift of the $I_c(H)$ dependence with respect to the $H = 0$ point. Therefore, at $H = 0$, for ideal $I_c(H)$ dependence, the I_c magnitude would be the same for the two opposite magnetization directions. In contrast, it is desirable to have two distinct levels of I_c at $H = 0$, which can be realized using a (pseudo-)spin valve.

The next generation of memory elements is based on MJJs where one uses a pseudo-spin valve (PSV) as a weak link sandwiched between the superconducting electrodes to allow for tunneling of the superconducting electrons [14–19]. At least two magnetic layers, F_1 and F_2, with a nonmagnetic spacer between them, are needed to realize a PSV in which one magnetic layer has lower coercive force than the other. This allows one to change the mutual orientation of the magnetization vectors in the $F_{1,2}$ layers by applying, e.g., a magnetic field. The proximity effect through this structure, and therefore, the associated magnitude of I_c depend on the mutual orientation of the magnetization vectors in PSV, which allows one to alter the magnitude of I_c in a controllable way.

Since magnetic materials are known to strongly suppress the superconducting correlations induced in them as a result of the proximity effect, the Josephson current density, j_c, through a (metallic) PSV serving as a barrier in MJJs is strongly reduced as compared with that in ordinary *SNS*, *SIS*, or *SNINS* junctions having comparable thicknesses of the nonmagnetic barrier material. Using a more sophisticated combination of magnetic materials for the barrier, assumed to enable the triplet pairing generation and long-range propagation of superconducting correlations [21], does not help to improve the situation [19]. Therefore, it is highly desirable to build a Josephson memory element in which a high j_c and a critical voltage $V_c \sim 1$ mV is realized in the Josephson junction in order to make it compatible with the SFQ logic. Motivated by this, we explore a memory element based on a multi-terminal superconducting-ferromagnetic device [22,23]. The principle of operation of our device is similar to proposals [4,11]; we exploit reversal of magnetization of a "free" magnetic layer in a PSV in order to control the magnitude of I_c in an adjacent (sensor) Josephson junction. However, unlike the behavior reported in [11], we observe *controllable* and *reproducible* change of the magnitude of I_c when reversing the magnetization direction of the "free" magnetic layer without irreversible latching of the critical current in one of the two states.

II. EXPERIMENT

The devices are fabricated from Nb/Al/AlO_x/Al/Nb/Al/Py/Al/AlO_x/Al/Ni/Al/Nb structures deposited onto oxidized Si substrates using the dc magnetron sputtering of the respective materials and thermal oxidation to form the AlO_x tunnel barriers. The thicknesses d_{Nb} of the bottom, middle, and top Nb electrodes are 120, 35, and 68 nm, respectively. The thickness of the middle Nb layer is chosen to be considerably less than the London penetration depth in the Nb films at 4.2 K (which is typically 80–100 nm in our films). The thickness of the Al overlayer used to form the AlO_x tunnel barrier is 9 nm. The four-terminal devices are patterned using an optical lithography, ion milling, reactive ion etching, anodization, and deposition of SiO_2 insulation.

Here, we consider devices where the thickness, d_{Py}, of the permalloy (Py, 80%Ni-20%Fe) "soft" magnetic layer is 5.0 nm, whereas the thickness, d_{Ni}, of the "harder" Ni layer is 4.7 nm. Therefore, the magnetic tunnel junction (MTJ) Py/Al/AlO_x/Al/Ni forms a PSV. The nominal lateral dimensions of the sensor (SIS') and the magnetic ($S'FIFS$) junctions are $W \times L = 2 \times 4\ \mu m^2$ and $W \times W = 2 \times 2\ \mu m^2$, respectively. The schematic view of the device structure and its biasing is shown in Fig. 1(a). Figure 1(b) shows a scanning electron microscope (SEM) image of an actual device (top view); the magnetic field was applied in the plane of the image in the top-down direction.

The devices are characterized in liquid He at 4.2 K. Current-voltage characteristics (I-V curves) and the dependences of the maximum Josephson current vs external magnetic field applied parallel to the layers' plane [$I_c(H)$ dependences] are measured.

I-V curves for a typical device are shown in Fig. 2. The sensor (Nb/Al/AlO_x/Al/Nb) junction is a Josephson junction, as is shown by the blue $I_s(V_s)$ curve. The magnetic

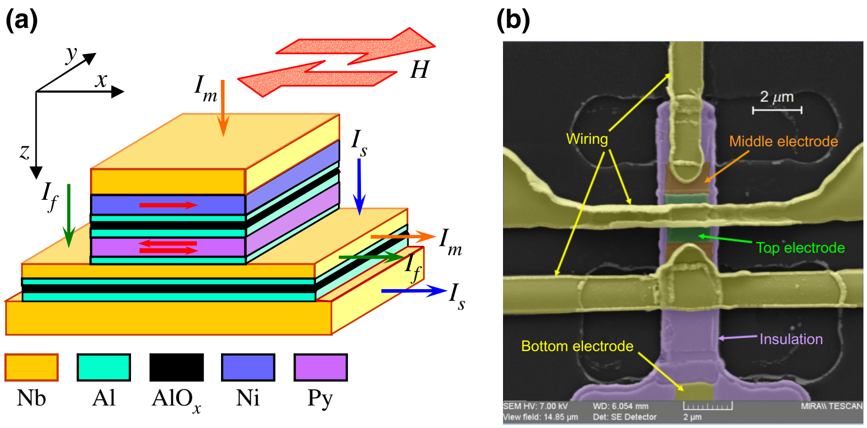

FIG. 1. (a) Schematic view of an $SIS'F_1IF_2S$ device and its biasing. (b) Scanning electron microscope micrograph of an actual four-terminal Nb/Al/AlO_x/Al/Nb/Al/Py/Al/AlO_x/Al/Ni/Al/Nb device. The magnetic field is applied in the plane in the top-down direction.

(Nb/Al/Py/Al/AlO_x/Al/Ni/Al/Nb) junction that represents a PSV is a *NIN* type junction (see red $I_m(V_m)$ curve). Also shown is the *I*-*V* curve of the middle Nb film (black $I_f\,(V_f\,)$ curve), which is superconducting.

Magnetization reversal is accomplished by an external magnetic field applied parallel to the structure plane as shown in Fig. 1. In order to properly determine the magnetic field sweeping range, we have fabricated a 5×10 mm^2 array of 2×2 μm^2 pillars made of the same multilayer structures as the devices themselves, and measured its magnetic moment vs field [$M(H)$] dependence at 10 K (just above the T_c of Nb). (Note that the pillars have the same size as that of the magnetic junctions in our devices). The $M(H)$ dependence is shown in Fig. 3(a); one can infer different coercivities of the Ni and Py layers.

Below we consider $I_c(H)$ dependence for one of our devices. Similar behavior is observed for several other devices. We prepared an initial magnetic state of the system by applying the field $\mu_0 H \approx +59$ mT, and then measured the $I_c(H)$ dependence within different ranges of H sweeping starting from low fields. Within the ranges below ± 4.5 mT, the $I_c(H)$ dependence is essentially the same for the two directions of H sweeping. Above that

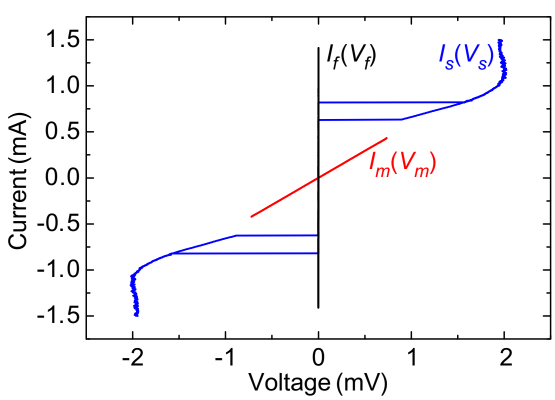

FIG. 2. *I*-*V* curves of the sensor (blue $I_s(V_s)$ curve) and the magnetic junction (red $I_m(V_m)$ curve); also shown is the *I*-*V* curve of the middle Nb film (black $I_f\,(V_f\,)$ curve).

field, the $I_c(H)$ dependence becomes hysteretic and manifests two distinct levels of maximum I_c for sweeping H in the two opposite directions. The maximum hysteresis is achieved in the sweeping range of $\mu_0 H = \pm 13.9$ mT; this dependence is shown in Fig. 3(b), where the two traces are denoted by red and black colors (lower and upper curves, respectively). The dependence is reproducible when it is recorded several times. The I_c reduction for the red curve is about 11% as compared to the black curve. This ratio can be increased in optimized devices. In particular, the parameters of the ferromagnetic layers have to be chosen so as to achieve full compensation of magnetic moments of the $F_{1,2}$ layers in the AP configuration.

One can see that there is correlation between the field range in which the maximum change of I_c is observed and the field where Py magnetization switching occurs [this field interval of about 9.0 mT is denoted by vertical blue dashed lines in Figs. 3(a) and 3(b)]. At the same time, in the sweeping range of $\mu_0 H = \pm 13.9$ mT, the Ni layer remains in essentially the same magnetization state [this sweeping range is denoted in Fig. 3(a) by two vertical red dashed lines]. We, therefore, conclude that the occurrence of two different maximum I_c levels for the black and red curves in Fig. 3(b) is associated with magnetization reversal of the Py layer.

We have carried out auxiliary experiments in order to determine the saturation magnetization, M_s, of the ferromagnetic layers in our structures. Specifically, we have measured magnetic moment vs parallel magnetic field [$M(H)$] dependence for Nb/Al/AlO_x/Al/Nb/Al/Py/Al/AlO_x/Al/Ni/Al/Nb, Nb/Al/AlO_x/Al/Nb/Al/Py/Al/AlO_x, and Nb/Al/AlO_x/Al/Nb/Al/Ni/Al/AlO_x structures with $d_{Py} = 5$ nm and $d_{Ni} = 4.7$ nm. From these measurements, we have determined M_s values of 0.571 and 0.365 T for Py and Ni, respectively.

Furthermore, we have measured $M(H)$ dependence at 4.2 K in the magnetic field applied perpendicularly to the film plane for Nb films with thicknesses of 35 and 100 nm in order to determine the critical fields H_{c1} and H_{c2}. These measurements reveal that the $\mu_0 H_{c1}$ field is about

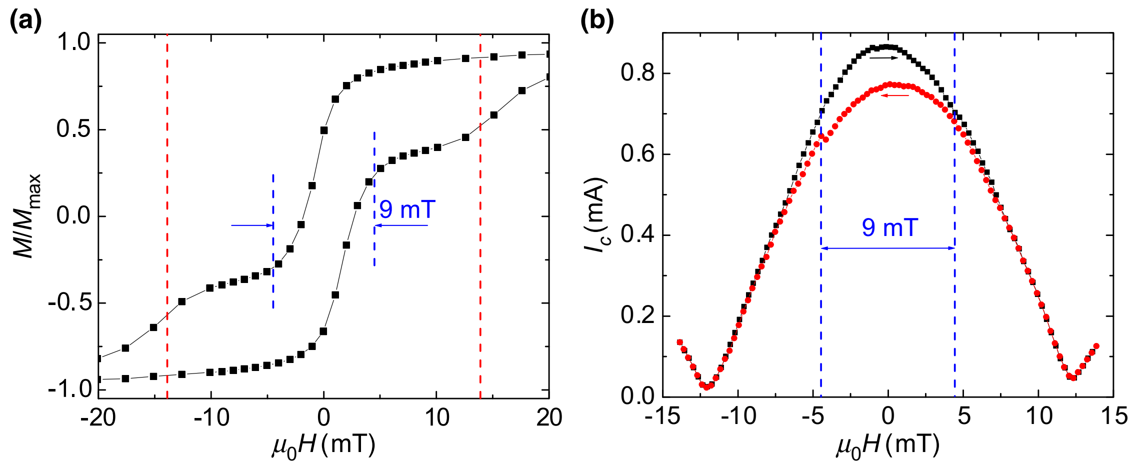

FIG. 3. (a) $M(H)$ dependence at 10 K for a 5×10 mm^2 array of 2×2 μm^2 pillars made of the same structure as the four-terminal devices. Red dashed lines denote the range of H sweeping in panel (b). (b) $I_c(H)$ dependence for the sensor junction in a four-terminal $SIS'F_1IF_2S$ device while sweeping an external in-plane magnetic field in two opposite directions in the range of ± 13.9 mT after initializing the magnetic state of the device at $\mu_0 H \approx +59$ mT. A significant change in I_c in the range of $\mu_0 H \approx \pm 4.5$ mT corresponds to the most significant change in magnetic moment of Py [see panel (a)].

3.5 mT for $d_{\rm Nb} = 35$ nm and about 6 mT for $d_{\rm Nb} = 100$ nm, whereas the $\mu_0 H_{c2}$ field is about 1 T for both films.

III. DISCUSSION

In order to better understand the observed behavior, we have fabricated and studied similar devices but with an "inverse" geometry: a smaller *S′IS* Josephson junction is situated on top of a larger PSV [24]. In this configuration, the influence of the perpendicular fringe field from the MTJ on the *SIS* junction is excluded; only a stray magnetic field can penetrate the *SIS* junction from its edges. The resultant effect of the PSV on the *SIS* junction is only a *shift* of the Fraunhofer pattern $I_c(H)$ along the H axis [for all $I_c(H)$ measurements, the external magnetic field H is applied parallel to the plane of the device electrodes], but no change in the maximum I_c magnitude is observed. This complementary experiment confirms that in the devices described here, the main effect of the PSV is a perturbation of the Josephson current by the fringe field penetrating the *SIS′* junction in the direction perpendicular to the planes of the *S* electrodes.

The influence of a perpendicular field on the *SIS* junction was previously investigated both theoretically and experimentally [11,25–29]. Since the perpendicular H_{c1} field in typical superconducting films is quite low (see experimental data for our Nb films above), they can easily trap Abrikosov vortices. Analysis [25] indicates that Abrikosov vortices trapped in the superconducting electrode(s) may influence the Josephson current of a *SIS* junction via two basic mechanisms: the "core" and "electrodynamic" mechanisms. The first mechanism means the suppression of superconductivity in a region on the order of the coherence length near the vortex core. The second mechanism modifies the Josephson current through a coordinate dependence of the gauge-invariant phase difference ϕ of the order parameters of the electrodes according to the basic relation $\nabla\phi = 2\pi\Lambda/\Phi_0[\mathbf{B} \times \mathbf{z}_0]$, where Λ is the magnetic thickness of the junction and $\mathbf{z}_0$ is the unit vector perpendicular to the plane of the junction [27].

It is shown [11,25–29] that trapping even one Abrikosov vortex in the superconducting electrode(s) may dramatically modify the $I_c(H)$ dependence, specifically, I_c may be close to zero at $H = 0$. In our case of randomly chosen thicknesses $d_{\rm Ni}$ and $d_{\rm Py}$, magnetic moments of the Ni and Py layers do not compensate each other in the AP state [see Fig. 3(a)]; there is always some field that affects the *SIS′* junction, and therefore, we do not know the magnitude of the Josephson current in a zero PSV field. This complicates the analysis of the influence of the PSV on the Josephson current. A simplified estimation of the orthogonal fringe field magnitude, H_z, at the surface of the S' layer in our structures can be made using the approach [5,6]. For the case of PSV, H_z can be expressed as $\mu_0 H_z = 2\bar{M}_s d_F z/(x^2 + z^2)$, where $\bar{M}_s$ is an effective saturation magnetization of PSV, d_F is its thickness, z is measured from the midpoint of the bilayer, and x is measured from its edge in the plane. For the P state, $\bar{M}_s$ is given as $\bar{M}_S^{\rm (P)} = (M_S^{\rm (Py)} d_{\rm Py} + M_S^{\rm (Ni)} d_{\rm Ni})/(d_{\rm Py} + d_{\rm Ni})$ [6]; for the AP state, we use $\bar{M}_S^{\rm (AP)} = (M_S^{\rm (Py)} d_{\rm Py} - M_S^{\rm (Ni)} d_{\rm Ni})/(d_{\rm Py} + d_{\rm Ni})$. This gives peak values $\mu_0 H_z \approx 1.9$ T for P and $\mu_0 H_z \approx 0.5$ T for AP states on the surface of S' beneath the PSV edges (i.e., at a distance $\Delta x = \pm 1$ μm from the center of PSV). Since the critical $\mu_0 H_{c2}$ field for our films is approximately 1 T, in the P state, the superconductivity of small areas of the S' layer just beneath the edges of the PSV may be suppressed due to penetration of the Abrikosov vortices (because the Nb films are type II superconductors). The Abrikosov vortices can also be formed in the AP state. Since both Nb films forming the electrodes of the SIS' junction are thinner than $2\lambda_L$ (where $\lambda_L \sim 100$ nm is the London penetration depth), we suggest that the Abrikosov vortices penetrate both films, and the magnetic force lines close outside of the SIS' junction. In this case, there is no phase shift due to the lateral field (because it is negligible inside the SIS' junction), and due to the nominal symmetry of the structure, the $I_c(H)$ dependence is symmetric. Therefore, the superconductivity is depressed in a small area of the S' and S electrodes along the PSV edges. However, the S' electrode remains superconducting [see curve $I_f(V_f)$ in Fig. 2], which implies that the actual influence of the fringe field may be not as strong as follows from the simplified expression for H_z used above.

Nevertheless, the physical mechanism of the I_c suppression suggested above is in qualitative agreement with our observations and explains why the difference in I_c is not very large for AP and P states, and why the $I_c(H)$ dependence is almost symmetric for both states. It follows from this analysis that separation between the two I_c levels for AP and P states can be increased in such devices, first, by appropriate choice of the d_{Ni} and d_{Py} so that the PSV does not induce any field outside in the AP state, and second, by making the device smaller. In the latter case, the area affected by the fringe field would be larger relative to the total area of the SIS' junction.

For the reasons mentioned above, we believe that our device has good prospects for scaling down to submicrometer dimensions. It is shown experimentally that submicrometer magnetic particles placed on top of an SIS junction can induce a high enough magnetic field to significantly modify the $I_c(H)$ dependence [11,30]. This implies that the device's lateral dimensions can be reduced to submicrometer size. If the ferromagnetic layers in a PSV are magnetized perpendicularly to the layers' planes, then a considerably stronger perpendicular field can be induced, and therefore, a stronger effect on the SIS junction can be obtained, which will allow for further reduction of the device dimensions.

IV. CONCLUSION

The most important result of this work is the demonstration of the possibility to control the Josephson current in an SIS junction in a reproducible manner using the magnetization reversal in an adjacent PSV. We observe two distinct values of maximum I_c for the SIS' sensor junction in four-terminal $SIS'F_1IF_2S$ devices due to magnetization reversal in the F_1IF_2 pseudo-spin valve while sweeping the external magnetic field in the opposite directions. Such switching can be done reproducibly without any latching of I_c in one of the states due to trapping of the Abrikosov vortices. Although in current devices the magnetization reversal is accomplished using an external magnetic field, potentially, it could be done using the electric current in two ways: first, by inducing the magnetic field while passing the current through the properly connected wiring layers, and second, by passing the electric current through the magnetic junction in order to exploit the spin-transfer torque mechanism [31,32]. In contrast to earlier work on spin-transfer torque switching of an MJJ [33], the multiterminal configuration of our device allows one to run the control current inducing the magnetization reversal only through the PSV without forcing the SIS junction into a resistive state.

We conclude that the $SIS'F_1IF_2S$ device can serve as a memory element in cryogenic computers. In comparison with the magnetic Josephson junctions developed by other groups, an advantage of our devices is that the SIS' junction can have Josephson critical current density and critical voltage of about 1 mV comparable to the respective values in SIS junctions exploited in SFQ circuits. Furthermore, the device can serve not only as a memorizing element, but as a complete memory cell involving both the memorizing element and the integrated readout element similar to [4]. This provides a significant advantage for achieving much higher density cryogenic memory arrays which are currently limited by the SQUID-based readout elements occupying more than 90% of the area of a memory cell.

ACKNOWLEDGMENTS

I.P.N. acknowledges using the facilities in Professor J. B. Ketterson's laboratory in the Department of Physics and Astronomy, Northwestern University. The authors acknowledge technical assistance rendered by Dr. O. Chernyashevskyy and useful discussions with Dr. S. E. Shafraniuk.

[1] M. A. Manheimer, Cryogenic computing complexity program: Phase 1 Introduction, IEEE Trans. Appl. Supercond. **25**, 1301704 (2015).
[2] O. A. Mukhanov, Energy-efficient single flux quantum technology, IEEE Trans. Appl. Supercond. **21**, 760 (2011).
[3] I. I. Soloviev, N. V. Klenov, S. V. Bakurskiy, M. Yu. Kupriyanov, A. L. Gudkov, and A. S. Sidorenko, Beyond Moore's technologies: Operation principles of a superconductor alternative, Beilstein J. Nanotechnol. **8**, 2689 (2017).
[4] T. Inoue, Superconductor magnetic memory cell and the method of accessing the same, US Patent 5276638 (1994).
[5] T. W. Clinton and M. Johnson, Nonvolatile switchable Josephson junctions, J. Appl. Phys. **85**, 1637 (1999).
[6] T. W. Clinton and M. Johnson, Magnetoquenched superconducting valve with bilayer ferromagnetic film for uniaxial switching, Appl. Phys. Lett. **76**, 2116 (2000).

[7] S. Oh, D. Youm, and M. R. Beasley, A superconductive magnetoresistive memory element using controlled exchange interaction, Appl. Phys. Lett. **71**, 2376 (1997).

[8] J. Y. Gu, C.-Y. You, J. S. Jiang, J. Pearson, Ya. B. Bazaliy, and S. D. Bader, Magnetization-Orientation Dependence of the Superconducting Transition Temperature in the Ferromagnet-Superconductor-Ferromagnet System: CuNi/Nb/CuNi, Phys. Rev. Lett. **89**, 267001 (2002).

[9] P. V. Leksin, N. N. Garif'yanov, I. A. Garifullin, J. Schumann, H. Vinzelberg, V. Kataev, R. Klingeler, O. G. Schmidt, and B. Büchner, Full spin switch effect for the superconducting current in a superconductor/ferromagnet thin film heterostructure, Appl. Phys. Lett. **97**, 102505 (2010).

[10] R. Held, J. Xu, A. Schmehl, C. W. Schneider, J. Mannhart, and M. R. Beasley, Superconducting memory based on ferromagnetism, Appl. Phys. Lett. **89**, 163509 (2006).

[11] A. V. Samokhvalov, S. N. Vdovichev, B. A. Gribkov, S. A. Gusev, A. Yu. Klimov, Yu. N. Nozdrin, V. V. Rogov, A. A. Fraerman, S. V. Egorov, V. V. Bol'ginov, A. B. Shkarin, and V. S. Stolyarov, Properties of Josephson junctions in the nonuniform field of ferromagnetic particles, JETP Lett. **95**, 104 (2012).

[12] T. I. Larkin, V. V. Bol'ginov, V. S. Stolyarov, V. V. Ryazanov, I. V. Vernik, S. K. Tolpygo, and O. A. Mukhanov, Ferromagnetic Josephson switching device with high characteristic voltage, Appl. Phys. Lett. **100**, 222601 (2012).

[13] I. A. Golovchanskiy, V. V. Bol'ginov, V. S. Stolyarov, N. N. Abramov, A. Ben Hamida, O. V. Emelyanova, B. S. Stolyarov, M. Yu. Kupriyanov, A. A. Golubov, and V. V. Ryazanov, Micromagnetic modeling of critical current oscillations in magnetic Josephson junctions, Phys. Rev. B **94**, 214514 (2016).

[14] C. Bell, G. Burnell, C. W. Leung, E. J. Tarte, D. J. Kang, and M. G. Blamire, Controllable Josephson current through a pseudospin-valve structure, Appl. Phys. Lett. **84**, 1153 (2004).

[15] B. Baek, W. H. Rippard, S. P. Benz, S. E. Russek, and P. D. Dresselhaus, Hybrid superconducting-magnetic memory device using competing order parameters, Nat. Commun. **5**, 3888 (2014).

[16] M. A. E. Qader, R. K. Singh, S. N. Galvin, L. Yu, J. M. Rowell, and N. Newman, Switching at small magnetic fields in Josephson junctions fabricated with ferromagnetic barrier layers, Appl. Phys. Lett. **104**, 022602 (2014).

[17] B. M. Niedzielski, E. C. Gingrich, R. Loloee, W. P. Pratt, and N. O. Birge, S/F/S Josephson junctions with single-domain ferromagnets for memory applications, Supercond. Sci. Technol. **28**, 085012 (2015).

[18] N. Banerjee, J. W. A. Robinson, and M. G. Blamire, Reversible control of spin-polarized supercurrents in ferromagnetic Josephson junctions, Nat. Commun. **5**, 4771 (2014).

[19] W. M. Martinez, W. P. Pratt, Jr., and N. O. Birge, Amplitude Control of the Spin-Triplet Supercurrent in S/F/S Josephson Junctions, Phys. Rev. Lett **116**, 077001 (2016).

[20] T. Golod, A. Iovan, and V. M. Krasnov, Single Abrikosov vortices as quantized information bits, Nat. Commun. **6**, 8628 (2015).

[21] F. S. Bergeret, A. F. Volkov, and K. B. Efetov, Long-Range Proximity Effects in Superconductor-Ferromagnet Structures, Phys. Rev. Lett. **86**, 4096 (2001).

[22] I. P. Nevirkovets, O. Chernyashevskyy, G. V. Prokopenko, O. A. Mukhanov, and J. B. Ketterson, Superconducting-ferromagnetic transistor, IEEE Trans. Appl. Supercond. **24**, 1800506 (2014).

[23] I. P. Nevirkovets, S. E. Shafraniuk, O. Chernyashevskyy, D. T. Yohannes, O. A. Mukhanov, and John B. Ketterson, Critical current gain in high-j_c superconducting-ferromagnetic transistors, IEEE Trans. Appl. Supercond. **26**, 1301907 (2016).

[24] I. P. Nevirkovets, S. E. Shafraniuk, and O. A. Mukhanov, Multiterminal superconducting-ferromagnetic device with magnetically tunable supercurrent for memory application, IEEE Trans. Appl. Supercond. **28**, 1800904 (2018).

[25] A. A. Golubov and M. Yu. Kupriyanov, Effect of single Abrikosov vortices on the properties of Josephson tunnel junctions, Sov. Phys. JETP **65**, 849 (1987).

[26] A. A. Golubov and M. Yu. Kupriyanov, Theoretical investigation of Josephson tunnel junctions with spatially inhomogeneous superconducting electrodes, J. Low Temp. Phys. **70**, 83 (1988).

[27] A. V. Samokhvalov, Current-phase relation in a Josephson junction coupled with a magnetic dot, Phys. Rev. B **80**, 134513 (2009).

[28] Q. Li, J. R. Clem, and D. K. Finnemore, Nucleation and motion of an isolated Abrikosov vortex, Phys. Rev. B **43**, 12843 (1991).

[29] R. Cristiano, L. Frunzio, S. Pagano, V. G. Palmieri, and M. P. Lisitskii, Experimental estimation of the hot spot size in Nb-based Josephson tunnel junctions using Abrikosov vortices, J. Appl. Phys. **82**, 5024 (1997).

[30] A. A. Fraerman, B. A. Gribkov, S. A. Gusev, A. Yu. Klimov, Yu. N. Nozdrin, V. V. Rogov, A. V. Samokhvalov, S. N. Vdovichev, L. Fritzsch, E. Ili'chev, and R. Stolz, Magnetization controlled effects in overlap Josephson junctions coupled with submicron magnetic dots, J. Phys.: Conf. Series **97**, 012233 (2008).

[31] J. C. Slonczewski, Current-driven excitation of magnetic multilayers, J. Magn. Magn. Mater. **159**, L1 (1996).

[32] J. A. Katine, F. J. Albert, R. A. Buhrman, E. B. Myers, and D. C. Ralph, Current-Driven Magnetization Reversal and Spin-Wave Excitations in Co/Cu/Co Pillars, Phys. Rev. Lett. **84**, 3149 (2000).

[33] B. Baek, W. H. Rippard, M. R. Pufall, S. P. Benz, S. E. Russek, H. Rogalla, and P. D. Dresselhaus, Spin-Transfer Torque Switching in Nanopillar Superconducting-Magnetic Hybrid Josephson Junctions, Phys. Rev. Applied **3**, 011001 (2015).